METALS AND MATERIALS, Vol. 4, No. 6 (1998), pp. 1111~1118

Physical and Mathematical Modeling of Metal Flow in the Continuous Casting of Steel and Aluminum

J. W. Evans, D. Xu and W. K. Jones, Jr.

Department of Materials Science and Mineral Engineering, University of California
Berkeley, CA 94720, USA

For a long time it has been recognized that flow of metal in the liquid pool at the head of a continuous caster can have a significant effect on the operability of the caster and the quality of the steel produced. Poorly engineered flows can result in thinning of the shell produced in the mold, with consequent danger of breakouts, entrapment of inclusions or gas bubbles, as well as macrosegregation. There can be similar impacts of the flow in the DC casting of aluminum. Flows are controlled, in the case of steel casting, by the design of the submerged entry nozzle (SEN) and by auxiliary devices such as electromagnetic brakes and stirrers. In the case of aluminum casting, it is common practice to place a ceramic "bag" around the SEN to control the flow. Usually the design of these devices involves much empiricism; the metal pools are hot and difficult to access, and flow measurements are therefore difficult. Some use has been made of mathematical and physical models in developing flow control devices. The difficulty with the former is that the flows are turbulent and in a volume with an irregular geometry; consequently, model predictions are questionable unless tested in some way. Such testing can be done using physical models which can also provide their own insights into the nature of the flow. Unfortunately, most physical modeling of casters in the past has been qualitative, or semi-quantitative. The paper describes a project at Berkeley where quantitative results are being obtained from a physical model of a caster with the help of particle image velocimetry (PIV). In this technique (cross correlation PIV), a digital camera records an image of tracer particles scattered throughout the flow. A second image is recorded 33milliseconds later and the two digital images are interrogated by commercial software (Optical Flow Systems, Edinburgh, Scotland) to determine the motion of the particles from one image to the next and yield a vector map of the flow. The technique has been extended to yield time averaged velocity vectors for turbulent flows (the case in the casters and models) by ensemble averaging the vectors from many pairs of images. Water models, including full sized ones, have been constructed for steel and aluminum casters. Various SENs and bags can be used in the model and their effects measured by PIV. Results show that the orientation of the two ports at the bottom of the SEN has a strong effect on the flow in steel casting. The water model of the aluminum caster has shown the strong effect of the bag geometry, and of bag misalignment, on flow in the liquid pool. The commercial software FIDAP has been used to compute time averaged velocities in the physical models. Agreement between measurements and predictions varies from good to fair, depending on conditions.

Key words : water modeling, continuous casting, particle imaging velocimetry, steel, aluminum

1. INTRODUCTION

It has been generally recognized that what happens in the liquid pool in a continuous caster, especially in the region of the mold, has an important effect on the surface and internal quality of ingots [1-2]. In the conventional continuous casting process of steel, the casting speed is high (usually 1-3 m/min), therefore; control of fluid flow within the mold region has continued to be a major research area since the conception of this process. The most important component in the metal delivery during the continuous casting of steel is the submerged entry nozzle (SEN). The importance of the nozzle can be simplified into two factors. First, the nozzle design is the controlling factor of the flow patterns that develop in the liquid pool. Secondly, the nozzle is the easiest and most cost-effective component to modify in search of a proper casting procedure. It is for this reason that many research endeavors have focused on trying to characterize the flow associated with entry nozzles. When attempting to understand the behavior of a nozzle associated with an actual steel caster important limitations must be addressed such as the opacity and the high operational temperature of

liquid steel. These factors limit most visualization attempts to qualitative studies, which do not allow detailed information about the flow. The desire for more detailed information has led researchers to use physical and mathematical modeling techniques to simulate the actual casting. The present paper is a report of an on-going investigation using an innovative physical model to better describe the flow within the liquid pool of steel and aluminum casters.

Physical modeling, in particular water modeling, is widely used in simulating the behavior of liquid steel during the casting process [3-7]. Modeling with water may seem like an over simplification of the problem, however; it can be shown through the proper dynamic similarity that water adequately models liquid steel. Using such a working fluid as water directly reduces the two difficulties of modeling liquid steel flows. Water modeling also permits the study of flow phenomena that are difficult to mathematically model, such as flow oscillation. However, while traditional techniques, such as Pitot tubes, hot wire anemometer and dye tracing, have given quantitative values these are only point by point techniques. This greatly reduces the amount of information that will be obtained from a given experiment. In some investigations [8-9], point measurements have been made to determine velocities throughout the whole of a flow field, however; these measurements are exceptional rather than usual. There is therefore a motivation to develop a technique that does not suffer from the same limitations as the previous methods. Particle imaging velocimetry is a relatively new technique that has the advantage over other visualization techniques of having the ability to quantitatively describe an entire flow field plane by plane. The method of analysis, in the simplest terms, requires that the flow be well seeded with neutrally buoyant, highly reflective particles, which in turn are illuminated in the plane of interest. Then, two images of the section are taken at a well-defined time interval. The relative displacements of the particles are measured, and since the time interval is known the velocities can be directly calculated.

The purpose of this paper is to describe a method (PIV) that quantitatively characterizes the flow in an effort to discover how metal delivery systems effect the flow patterns in the mold region of a steel or aluminum caster.

2. EXPERIMENTAL PROCEDURE

A laboratory scale model of a caster was built and is sketched in Fig. 1. The system consists of a Lexan tank,

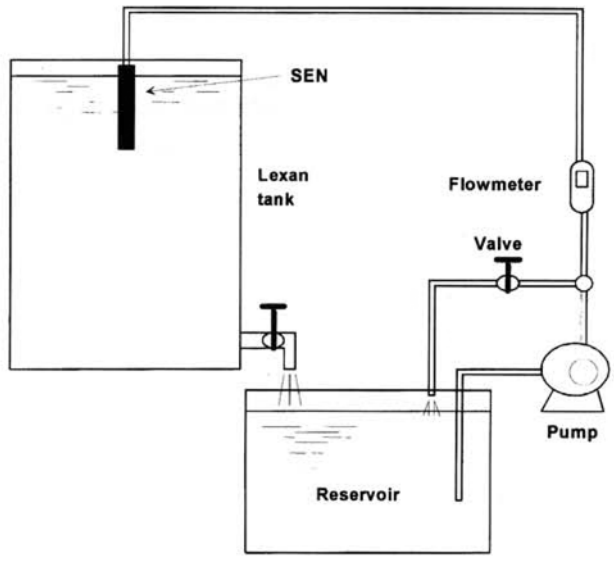

Fig. 1. Illustration of the physical model using the current study.

with dimensions $0.762 \times 0.152 \times 1.02$ meters W/D/H, which serves as the mold walls, a submerged entry nozzle and a water delivery system. The nozzles used throughout this study are of the bifurcated type with varying angles of inclination from the horizontal for the centerline of the port. The nozzle has a port diameter of 25.4 mm and an internal diameter of 25.4 mm. Submergence depth was fixed at 160 mm for all cases presented. The flowrate at the nozzle port was calculated to be 9.12×10^{-4} m^3/sec. while the the injection rate of argon gas (when used) was 8.3×10^{-5} m^3/sec.

A PIV system consists of four essential components: an illumination source, particle seeding, image capturing hardware and the processing software. For this study a halogen light array was used instead of a costly laser light source. The light box that was designed consisted of three 1.5 kW light banks, which were highly collimated through an adjustable slit in the bottom of the box. This arrangement produced an intense sheet of light over the desired spatial area. The seeding particles used were made of latex and ranged from 200-300 μm in size. This material was chosen because it satisfied both important parameters which are that the seeding be neutrally buoyant in water and have a high reflectivity in the illumination plane. The images of the illumination plane were captured digitally using a CCD camera (Pulnix TM9700) and an image-grabbing board (BitFlow Raptor VS-4). The digital images were stored on a personal computer for subsequent processing. The software that was used to perform the correlation was developed by Optical

Flow Systems Limited.

3. RESULTS OF SIMULATIONS

3.1. Steel casters

The beginning of this study was limited to understanding the flows generated by different inclination angles of the SEN ports and the effects of argon injection. Figs. 2a-b shows vector maps generated for the case of 0° nozzle inclination. The view is of the left half of the model with the SEN on the right. The vertical plane shown ("central section") is parallel to the wide face of the caster and passed through the center of the nozzle. The turbulent nature of the flow is captured and is most easily interpreted by noticing that the two vector maps which vary only in time have considerably different flow patterns. The ability to capture instantaneous features of the flow is an important tool when one is interested in studying time variant processes, such as flow oscillations. However, for this study, the instantaneous results were not adequate due to the difficult task of comparing the physical results with ones calculated using standard time-averaged numerical techniques. Therefore, to remedy the situation, ensemble averaging of the instantaneous PIV result was performed. It was shown that averaging the velocities of 40 instantaneous PIV maps generated a map of the time-averaged nature of the flow. Fig. 3a is a time-averaged vector map (TAV) for the 0° inclination case. By effectively eliminating the variations in time, the TAV map can be tested against computational solutions found using standard time-averaged turbulent models.

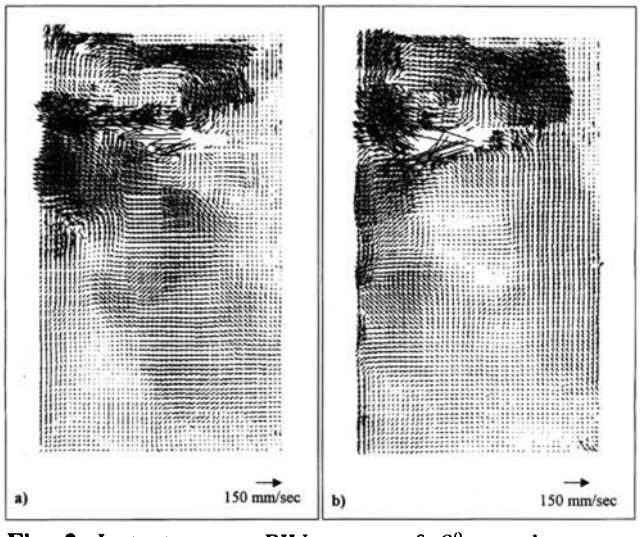

Fig. 2. Instantaneous PIV maps of 0° nozzle - central section.

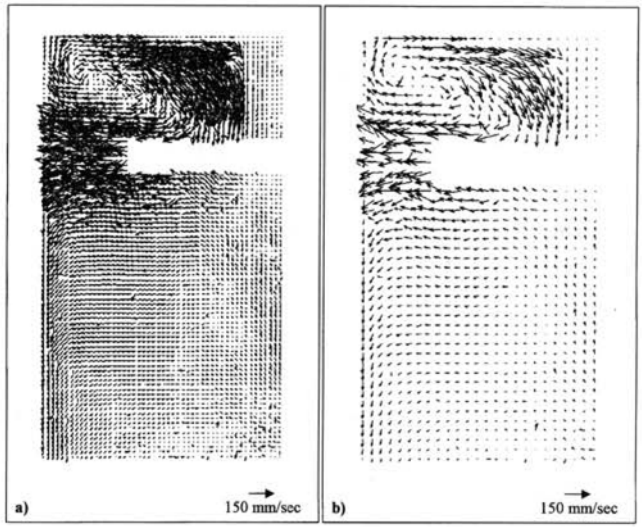

Fig. 3. TAV maps of 0° nozzle - central section (a) 8×8 grid, (b) 16×16 grid.

Figs. 3a-b shows two TAV maps of the central section of the 0° angle. The difference between the two figures is in the interrogation size used during the cross correlation. Fig. 3a was generated using a grid size of 8×8 pixels, while Fig. 3b was calculated using 16×16 pixels as a grid parameter. There is a slight loss of information in using a reduced number of grid points but the appearance of the flow remains intact. The obvious benefit, of using Fig. 3b to interpret that flow, is that it is easier to visualize and for that reason all images shown in this study will be processed with the same grid spacing as Fig. 3b. It must be noted that the highest velocity vectors, ones generated closest to the exit of the nozzle, are not captured. This is simply due to using a digital camera that does not have a fast enough framing speed. In the instantaneous maps, such as Fig. 3a, several of the high-speed vectors are noticeable, however when the ensemble averaging is performed these vectors are removed in the areas that are shown blank.

The flow in Fig. 3 is best described as two counter rotating loops, with the smaller loop near the surface. This flow is not surprising for the 0° nozzle. Fig. 4 shows the flow in the quarter section (half way between the central section and the wall) for the same experimental setup. The flow is significantly different from that shown in Fig. 3. This is mainly due to the jet from the ports of the nozzle not dominating the flow in this section, i.e. the outflow from the nozzle does not spread to considerably modify the flow pattern. Fig. 5 is a TAV

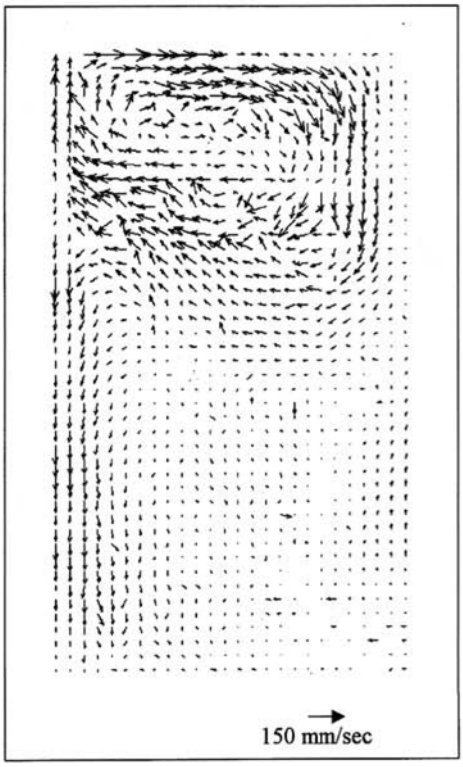

Fig. 4. TAV map of 0° nozzle - quarter section - no argon.

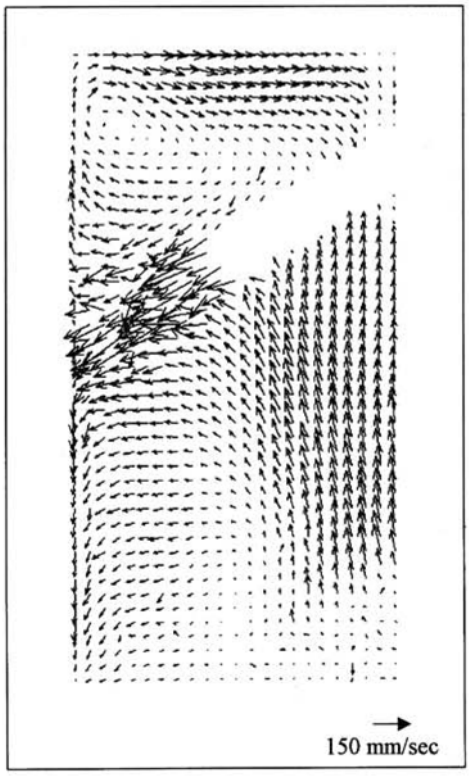

Fig. 5. TAV map of 30° nozzle - central section - no argon.

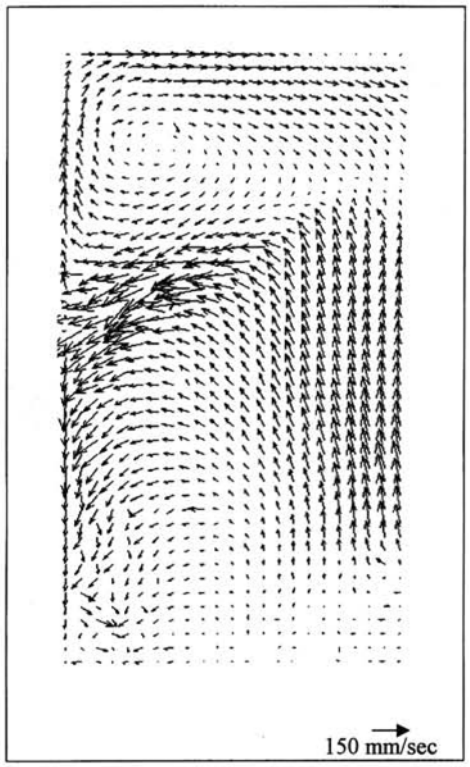

Fig. 6. TAV map of 30° nozzle - quarter section - no argon.

map of the central section of a 30° downward-inclined nozzle. It is evident from comparing Figs. 3 and 5 that the nozzle angle can greatly effect the flow in the mold region. The impingement point (i.e. the point of contact of the hot stream from the nozzle with the steel shell) of the flow is considerably deeper than in Fig. 3. Furthermore, the flow has a large section of strong recirculation along the centerline of the mold that was absent in the 0° nozzle. Fig. 6 shows the quarter section of the 30° nozzle. The flow is similar to that given for the central section; most importantly, that the jet from the nozzle is visible in the quarter section. This suggests that the flow from the nozzle does spread significantly into the bulk of the fluid. This is an interesting result as it is not shown to be the case in the 0° nozzle.

The effect of argon injection through the nozzles is also studied, although at this point of the study there is some concern regarding whether the current PIV technique is generating vector maps based on the seeding particles or the argon bubbles. It is therefore the belief that the maps are averages of both the fluid and bubbles, and still can be valuable in illustrating the flow. Fig. 7 shows the flow through the central section of a 0° nozzle with 5 L/min argon injection. The

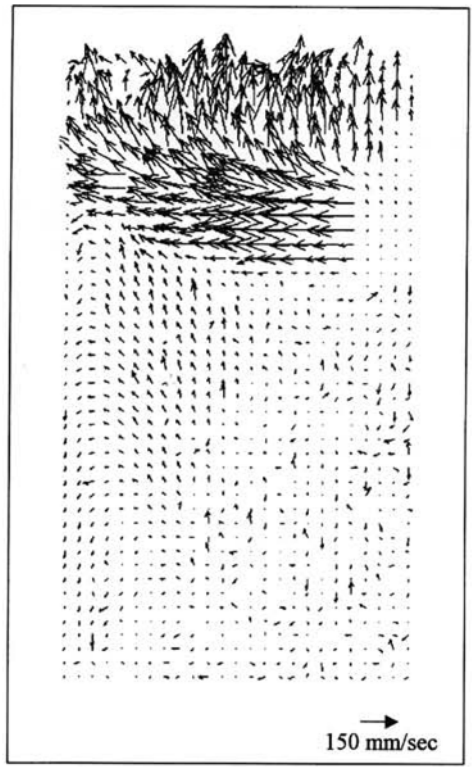

Fig. 7. TAV map of 0° nozzle - central section - 5L/min argon.

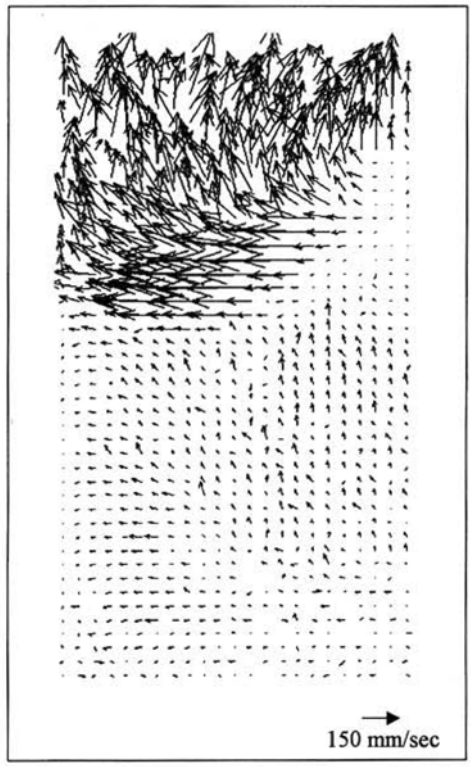

Fig. 8. TAV map of 30° nozzle - central section - 5L/min argon.

buoyancy induced flow of the bubbles serves to break up the two flow loops shown in Fig. 3. Although not directly shown it is important to note that the surface turbulence is enhanced due to the addition of bubbles into the flow. As expected, the argon flow has an even more pronounced effect on the flow generated through the 30° nozzle, as shown in Fig. 8. The depth into which the argon penetrates is greatly enhanced by the 30° downward nozzle, which gives rise to longer bubble residence times. However, this can be a disadvantage because in an actual caster it would lead to deeper penetration of the argon bubbles into the liquid steel possibly leading to high amounts of trapped argon bubbles in the cast steel.

Numerical calculations of the 3D turbulent flow have been performed using the commercially available finite element package, FIDAP. The model geometry and boundary conditions were representations of the physical model. The one difference in the model was that the free surface of the computational model was constrained, i.e. was not modeled as a deformable surface. Approximately 55,000 eight node linear elements were used to describe the nozzle and the mold regions. Convergence was obtained after 72 iterations. Fig. 9 shows the calculated

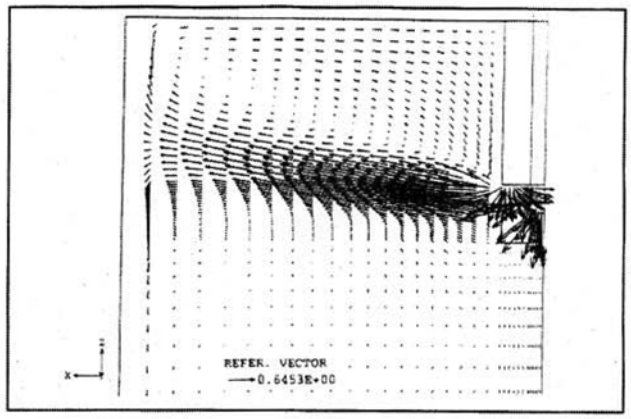

Fig. 9. Computed results of the 0° nozzle - central plane-no argon injection.

flow fields for the 0° nozzle in the central plane. The flow patterns are in good agreement with Fig. 3 although the magnitudes of the velocities are slightly higher in the computed results. Fig. 10 illustrates the flow profile in the quarter section for the 0° nozzle. The model calculations predict similar flow near the nozzle to that generated in the physical model. The magnitudes of the velocities in the computed and experimental results for the quarter plane are in accord.

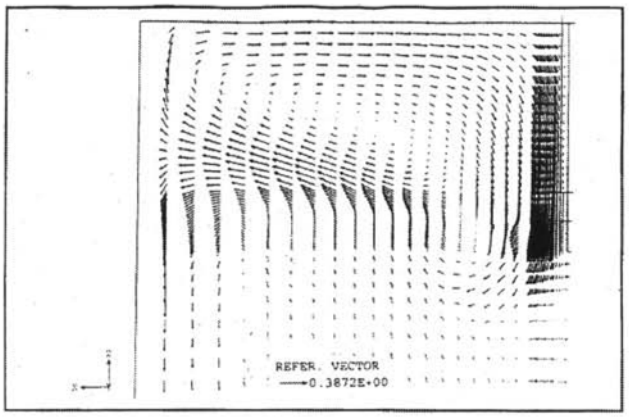

Fig. 10. Computed results of the 0° nozzle - quarter plane - no argon injection.

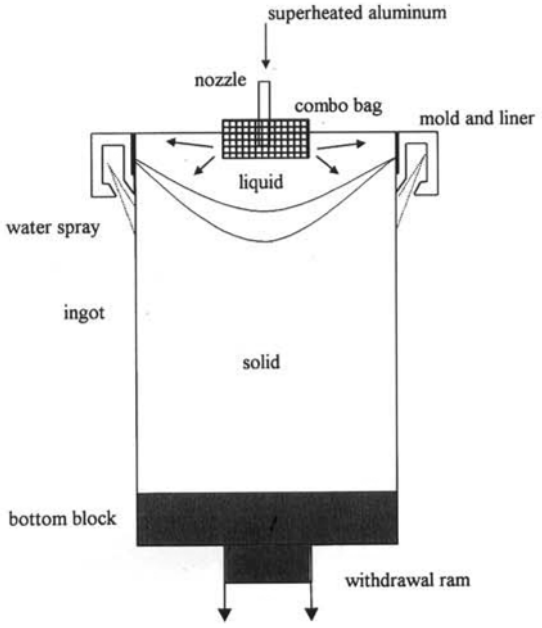

Fig. 11. Schematic of the DC casting process.

3.2. Aluminum casting

Much of the world's primary production of aluminum is cast into ingots using "direct chill" (DC) casting; this is sketched in Fig. 11. The DC casting technology is similar to the continuous casting of steel although there are some important differences. The mold is not oscillated in DC casting, the ingot descends into a casting pit without bending and the casting speeds are low (approximately 1 mm/s). Another important difference is in the way the molten metal enters the liquid pool at the head of the caster. Rather than using an SEN with ports to direct the metal horizontally towards the short sides of the caster (as in steel casting), the aluminum industry usually uses a "bag" of woven ceramic fibers to achieve the required

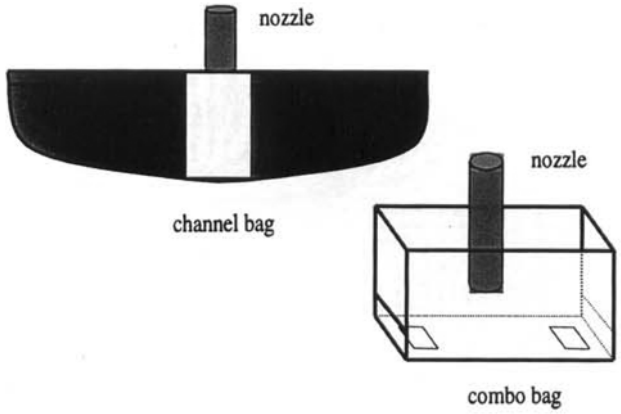

Fig. 12. Schematic of two different bag designs used in DC casting.

flow. Fig. 12 illustrates two typical bag designs. The "combo" bag is mostly of a closely woven material that is impermeable to aluminum but part of the bag is of a more open weave and aluminum flows readily through these "windows". Previously the design of these bags has been empirical and the aim of the work at Berkeley has been a more fundamental understanding of the effect of bag design and use on flow in the DC caster. As in the work on steel, a water model has been used (along with mathematical modeling) and velocities measured by PIV. The main difference from the water model for steel arises because the liquid pool is shallow (200-250 mm) in casting aluminum. The reader is referred to a recent publication [10] to learn how the pool was simulated.

Fig. 13 shows representative results for two cases. The upper half of the figure is the flow for no bag in the caster while the lower figure is for a combo bag (102 mm long) in place. The nozzle is at the upper right (shaded area in upper half), with the solidification front being the diagonal boundary from upper left to lower right. At each end of the combo bag (shaded area in lower half) there are two windows illustrated by the heavy dark lines. One half of the vertical plane through the caster is illustrated (the other half is symmetric) and the lengths of the arrows indicate the magnitudes of the time averaged velocities, with the scale at the lower left. Velocities just below the nozzle in the upper half of the figure are too high to be captured by the PIV system.

The presence of the bag is seen to radically alter the flow pattern in the simulated liquid metal pool. The strong downward flow beneath the nozzle, with its return flow upward and to the left along the solidification front, is eliminated when the bag is present. The flow with the bag present is a jet which moves downward and

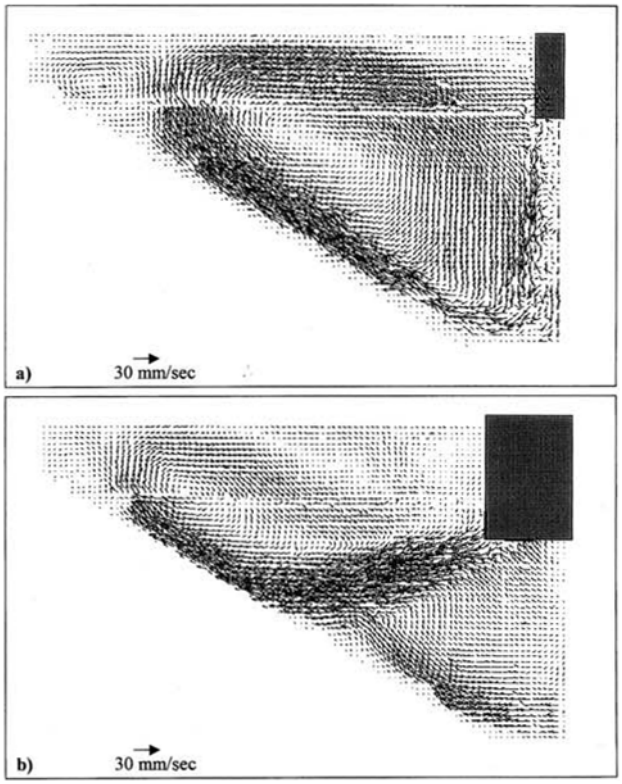

Fig. 13. PIV results of no bag and 102 mm combo bag.

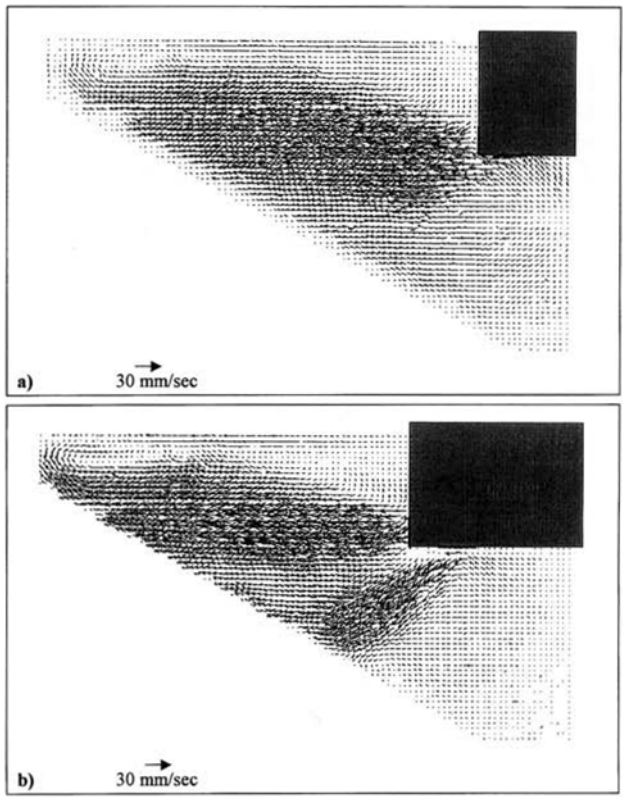

Fig. 14. PIV results of 152 and 203 mm combo bag.

outward from the end of the bag, striking the solidification front at mid-height. Fig. 14 gives the flow patterns that result from longer bags (152 mm in upper half and 203 mm in lower half). Comparing the two halves of this figure and the lower half of Fig. 13, it is seen that the length of the bag has a major influence on fluid flow. With the longest bag, the flows issuing from the two windows are separated. For other results on the effect of bag design, bag (mis) placement and nozzle position the reader is referred to recent papers [10,11].

4. CONCLUSIONS

The progress of ongoing research into metal delivery systems has been shown. The dependence of the flow pattern on the nozzle configuration (and bag configuration in the aluminum case) has been illustrated. The addition of argon gas to the model system has shown that it plays a crucial role in determining the dynamics of the flow in the mold region. The current physical modeling technique has shown itself stable, robust and reproducible. Several essential points need to be addressed to increase the capability of the PIV system. First, a CCD camera with a faster framing speed should be used in order to capture the flow around the nozzle region. Secondly, an effective method for distinguishing the bubble signals from that of the particle signals needs to be developed. This would allow measurements of only the flow during the argon injection experiments. Lastly, the addition of hot water into the system will allow for measurements of thermal buoyancy flows generated during casting. A method, using an inline heater, is under development.

ACKNOWLEDGMENT

Research supported by Reynolds Metals Company and The Aluminum Company of America.

REFERENCES

1. S. Yokoya, Y. Asako, S. Hara and J. Szekely, *ISIJ Int.* **34**, 883 (1994).
2. J. Herbertson, Q. L. He, P. J. Flint, R. B. Mahapatra, *Steelmaking Conf. Proc.* **74**, 171 (1991).
3. D. J. Harris and J. D. Young, *Steelmaking Conf. Proc.* **65**, 3 (1982).
4. D. Gupta and A. K. Lahiri, *Metall. Trans.* **27B**, 757 (1996).
5. X. K. Lan, J. M. Khodadadi and F. Shen, *Metall. Trans.*

28B, 321 (1997).
6. D. Gupta and A. K. Lahiri, *Metall. Trans.* **25B**, 227 (1994).
7. D. Gupta, S. Chakraborty and A. K. Lahiri, *ISIJ Int.* **37**, 654 (1997).
8. J. Szekely and R. T. Yadoya, *Metall. Trans.* **3**, 2673 (1972).
9. B. G. Thomas, X. Huang and R. C. Sussman, *Metall. Trans.* **25B**, 527 (1994).
10. D. Xu, W. K. Jones, Jr., J. W. Evans and D. P. Cook, in *Light Metals 1998* (ed., B. Welch), p. 1045, TMS, Warrendale, PA (1998).
11. W. K. Jones, Jr., D. Xu and J. W. Evans, in *Light Metals 1998* (ed., B. Welch), p. 1051, TMS, Warrendale, PA (1998).